J Mater Sci: Mater Electron (2023) 34:218

Fabrication of low-cost p-n heterostructure room temperature LPG sensing properties of Polyaniline–Copper ferrite composite

S. Kotresh[1], Aashis Roy[2,*], Ameena Parveen[3], Nacer Badi[4], and A. Murali[5]

[1] Department of Physics, Bangalore University, JB Campus, Bangalore 560056, Karnataka, India
[2] Department of Chemistry, S.S. Tegoor Degree College, Gubbi Colony 585104, Karnataka, India
[3] Department of Physics, Government First Grade College, Gurumitkal 585124, Karnataka, India
[4] Department of Physics, Faculty of Science, University of Tabuk, Tabuk 71491, KSA, Saudi Arabia
[5] School for Advanced Research in Polymers, Central Institute of Plastics Engineering & Technology (CIPET), Chennai 600032, India

Received: 6 August 2022
Accepted: 28 November 2022
Published online: 20 January 2023

ABSTRACT

The current study demonstrates the sensing response of a polyaniline–copper ferrite (PANI-$CuFe_2O_4$) nanostructured composite for liquefied petroleum gas (LPG) sensing. Fourier transform infrared spectroscopy (FTIR), X-ray diffraction (XRD), and scanning electron microscopy (SEM) techniques were used to characterize the PANI and the nanocomposite prepared by chemical polymerization method. At room temperature, a simple LPG sensor with a maximum sensing response of 86% at 764 ppm LPG was fabricated using only spin coated PANI-$CuFe_2O_4$ nanocomposite. It is observed that as the gas concentration in parts per million (ppm) increased, the composite's resistance also decreased. Their quick reaction and recovery durations, as well as their sensing performance stability, which are demonstrated their potential candidature for gas sensing applications. To describe how the sensing mechanism works, the p-n hetero-junction barrier produced at the interface of PANI and $CuFe_2O_4$ is used.

1 Introduction

Conducting polymers are the most intriguing materials because they combine the mechanical qualities of polymers with the electrical properties of metals and semiconductors, making them suitable for a wide range of technological applications, which including energy storages and various sensing applications [1–3]. Chemical stability and mechanical strength of these conducting polymers, on the other hand, are concerns. Many researchers have recently concentrated on the synthesis of organic–inorganic hybrid systems made up of metal oxides and conducting polymers to address these restrictions. The hybrids have also been proven to be well-known materials with promising applications in sensors, super

Address correspondence to E-mail: aashisroy@gmail.com

https://doi.org/10.1007/s10854-022-09662-z

capacitors, corrosion, solar cells, and light emitting diode devices [4–8] because of their versatility in altering electrical and mechanical properties to create desired synergistic effects Sensing applications are now being explored using hybrid heterojunctions-based nanocomposites [9–12].

In both household and industrial applications, highly flammable gases such as methane, butane, hydrogen, and LPG are routinely used and due to leakage of these flammable gases many incidents occurred. To save lives and property, it is critical to detect the leakage of such gases in lower concentration using extremely sensitive and highly responsive sensor devices [13, 14]. The goal of this study is to fabricate the organic–inorganic hybrid heterojunctions to produce at room-temperature operable LPG sensors. Polyaniline has unique electrical properties, environmental stability, and ease of processing, therefore we used as active layer in the sensor fabrication. Because it is a well-known geometrically frustrated system with good electrical, magnetic, and reducing gas sensing properties, $CuFe_2O_4$ nanoparticles are preferred as inorganic components. It has a characteristic spinel structure AB_2O_4 which belongs to the cubic space group, with Cu^{2+} ions filling the tetrahedral 'A' sites and Fe^{2+} ions filling with the octahedral B sites [15, 16]. We have synthesized PANI-$CuFe_2O_4$ nanocomposite employed for LPG sensing properties because of these favorable properties of both PANI and $CuFe_2O_4$. Furthermore, currently existing metal oxide sensors have two fundamental drawbacks: limited sensitivity and high working temperatures, both of which are undesirable. In addition, existing metal oxide sensors have two major flaws: low sensitivity and a high working temperature that consumes a lot of power, both of which are undesirable. Using p-type PANI and n-type $CuFe_2O_4$ to create a p-n heterojunction barrier that can function as an LPG sensor at room temperature, this work attempts to overcome some of the drawbacks of metal oxide sensors. The electrical, magnetic, and thermal properties of PANI-ferrite composites have been studied by a number of researchers. It's worth noting that the majority of these investigations on PANI-ferrite composite systems have focused on their magnetic, electrical and thermal properties, with only a few looking into their potential as gas sensors.

In this context, our research has a significant endeavor to fabricate a PANI-$CuFe_2O_4$ nanocomposite for LPG sensing properties in a practical manner. A low-cost spin coating procedure was employed to make the nanocomposite film, which was then subjected for LPG sensing. The creation of a p-n heterojunction barrier between p-type PANI and n-type $CuFe_2O_4$ is used to explain the mechanism of LPG sensing.

2 Experimental

2.1 Materials

Aniline ($C_6H_5NH_2$) (99.5%), ammonium persulphate [$(NH_4)_2S_2O_8$] (98%), hydrochloric acid (HCl) (34.5%), Copper nitrate [$Cu(NO_3)_2.4H_2O$] (99%), ferric nitrate [$Fe(NO_3)_3.9H_2O$] (99%) and urea (CH_4N_2O) (99.5%), all these reagents were purchased from S.D. Fine Chemicals, Mumbai, India.

2.2 Preparation of *n*-type $CuFe_2O_4$

The auto-combustion method was employed to prepare the n-type $CuFe_2O_4$ particles as mentioned earlier in the literature [19, 20]. The stoichiometric amounts of $Cu(NO_3)_2.4H_2O$, $Fe(NO_3)_3.9H_2O$, and CH_4N_2O were diffused into deionised water yielding a uniform solution. This step is done to trigger an exothermic reaction which is self-propagating in nature. The solution is then decanted into a silica crucible and ignited up to the temperature of 300 °C with a muffle furnace until the solution produces exhaustive gaseous products yielding ferrite nanoparticles in the form of powdered foam.

2.3 Preparation of PANI-$CuFe_2O_4$ nanocomposite

The PANI-$CuFe_2O_4$ nanocomposite was prepared by in situ polymerization method at room temperature as reported in earlier literature [4, 13, 21]. To start with, 6.7 ml aniline was dissolved in 180 ml of 1 M HCl taken in a 500 ml round bottomed flask and stirred well to which previously prepared $CuFe_2O_4$ powder (10 Wt. % with respect to aniline concentration) was added with vigorous stirring and then sonicated for 15 min to facilitate the adsorption of aniline on the $CuFe_2O_4$ surface. 7.5 g ammonium persulphate in 60 ml de-ionized water was added to this mixture, and it was allowed to polymerize for at

least 8 to 10 h with constant stirring. After filtration and multiple washings with distilled water and acetone, the composite was collected and dried in a vacuum oven at 100 °C for 8–10 h, yielding a dark green powder. Similarly, pure PANI was synthesized without $CuFe_2O_4$ under the same circumstances.

2.4 Mechanism of formation of PANI-$CuFe_2O_4$ nanocomposite

Figure 1 shows the PANI-$CuFe_2O_4$ nanocomposite preparation process. The presence of iron within the ferrite surface results in a positively charged surface with a point zero charge of pH 6 [17] in an acidic environment. To compensate for the positive charge, the anions (Cl^-) of HCl are adsorbed onto the ferrite surface. The aniline monomers converted into anilinium cations along this path, resulting in electrostatic interactions between the anions and the anilinium cations. The aniline monomers are electrostatically complex and surround the ferrite surface. By employing an oxidising agent like APS at room temperature, it will yield PANI-$CuFe_2O_4$ nanocomposite through polymerisation [18].

3 Characterizations

FTIR, XRD, SEM, and TEM techniques were used to characterize the produced samples. A Nicolet 750 spectrometer with a wave number range of 4000–400 cm^{-1} was used for FTIR spectroscopy. The diffractograms were recorded in terms of 2 in the range 10–80° using a Siemens D-5000 powder X-Ray diffractometer with CuK source radiation of wavelength 1.54°. A Hitachi S-520 scanning electron microscope was used to examine the composite's surface morphology. To avoid charging at the sample surfaces, each powder sample was spread on the surface of carbon tape fixed on an aluminum tab and conductive gold coated on the sample, and thus selected portions were photographed.

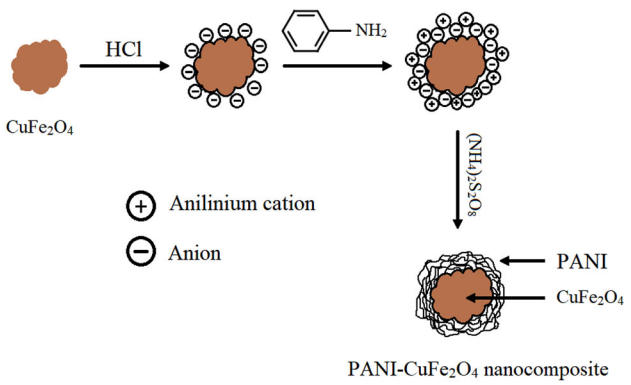

Fig. 1 Schematic diagram of formation PANI-$CuFe_2O_4$ composite

3.1 Fabrication of thin film

For sensing measurements, PANI and the composite film were developed by dissolving the sample in m-cresol and then coated on a glass plate in the shape of a film of about 2 µm thickness by spin coating unit (Make: Delta Scientific Pvt. Ltd, India, Model: Delta Spin I). Then, silver inter digitized electrodes were printed on film as shown in Fig. 2.

3.2 Sensor measurements

The film was positioned in an evacuated glass chamber at the top. The resistive type sensing response to LPG was carried out by using an electrometer (Make: Keithley, Germany, Model: 6517A. The LPG and test gases introduced from the bottom inlet fitted with a mass flow controller (Make: Alicat Technology, USA, Model: MC-SCCM 100-D/5 M, 5IN, RIN). The initial humidity in the chamber was measured around 32% which is removed with the help of vacuum pump and placed $CaCl_2$ salt into the bottom of the chamber to bring optimum level before experiments with LPG. The experimental setup used for the study at room temperature is shown in Fig. 3.

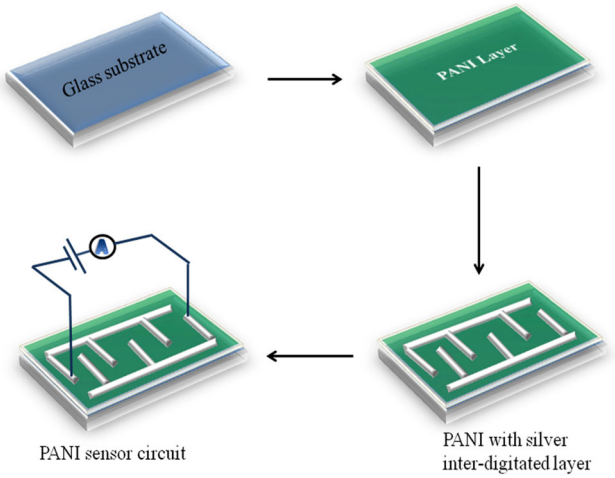

Fig. 2 Schematic illustration of thin film with interdigitated silver electrodes

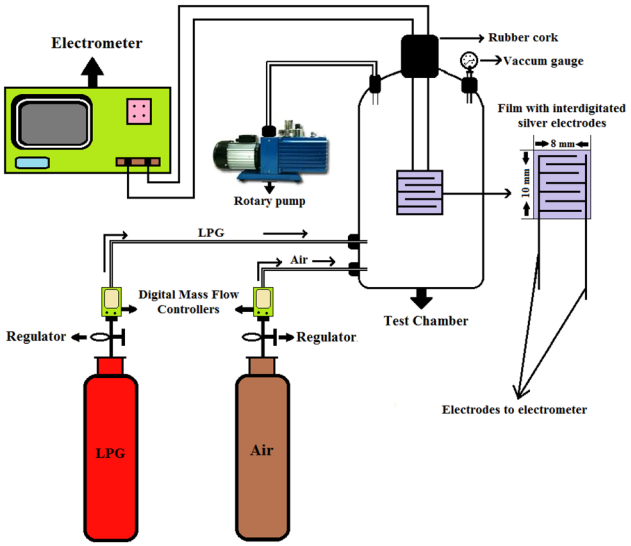

Fig. 3 The schematic diagram of experimental setup for gas sensing studies

4 Results and discussion

4.1 Fourier transform infrared spectroscopy

Figure 4 indicates the Fourier transform infrared spectroscopy (FTIR) spectra of PANI, PANI- $CuFe_2O_4$, and $CuFe_2O_4$. Figure 4(a) shows the spectra of PANI and the composites, the characteristic absorption bands of PANI occur at 797 cm^{-1}, 1138 cm^{-1}, 1238 cm^{-1}, 1301 cm^{-1}, 1492 cm^{-1}, 1575 cm^{-1} and 3446 cm^{-1} respectively. The broad band at 3446 cm^{-1} is attributed to O–H stretching of water molecules [22].

The bands that can be viewed 1575 cm^{-1} and 1492 cm^{-1} are the characteristic C = C stretching of the quinoid and benzenoid rings, the band at 1301 cm^{-1} and 1238 cm^{-1} are consigned to C–N stretching of the aromatic benzenoid rings, the broad band at 1138 cm^{-1} that is defined by MacDiarmid et al. as the "electronic–like band" is linked to the vibration mode of N = Q = N (here Q represents the quinoid ring), signifying the formation of HCl doped PANI [4, 22, 23], the band at 797 cm^{-1} is marked to the out of plane deformation of C–H in the 1,4–disubstituted benzene ring as shown in Fig. 4(b). The resultant stretching vibrations of PANI are in tune with published research studies [24, 25]. In any respect, the FTIR spectrum of the nanocomposite indicates a small shift substantiating the interfacial interaction within the ferrite particles and the PANI chains in both their respective bands. The PANI

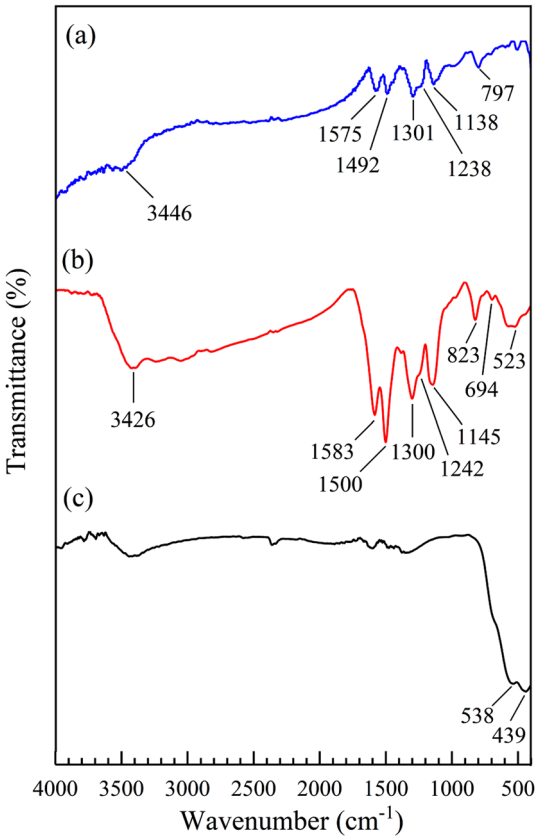

Fig. 4 FTIR spectra of **a** PANI **b** PANI- $CuFe_2O_4$, and **c** $CuFe_2O_4$

chains and the O-atoms share an H-bonding encircling the ferrite surface. This force is impelling and roots the ferrite particles into the PANI chains [27].

Waldron reported [19, 26], the ferrite metal ions are generally positioned in two different sub lattices assigned as tetrahedral and octahedral sites agreeing to the geometrical configuration of the oxygen nearest neighbors. Figure 4(c) shows the FTIR spectrum shows at 538 and 439 cm^{-1} corresponding bands of $CuFe_2O_4$, all samples with two significant Fe–O stretching vibrations in the spectrum, analogous to the intrinsic stretching vibrations that are seen at both the tetrahedral and the octahedral sites [28, 29]. The feature attributes of the spinel ferrites in single phase are outlined by the absorption bands.

4.2 X-ray powder diffraction technique

Figure 5 indicates the X-ray powder diffraction (XRD) patterns of PANI, PANI- $CuFe_2O_4$ composite and $CuFe_2O_4$. Figure 5(a) it is observed that the three diffraction peaks of PANI at $2\theta = 15.3^\circ$, 20.8° and 25.2° correspond to (100), (110) and (111) planes and

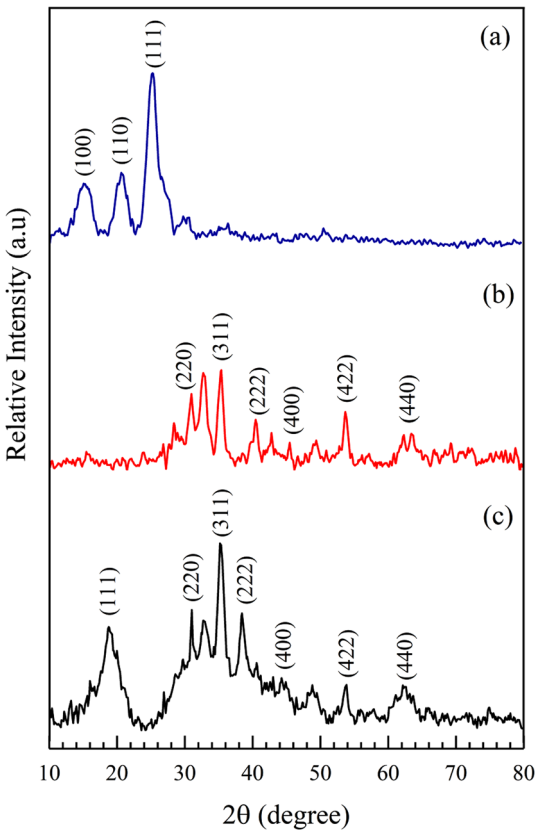

Fig. 5 XRD pattern of **a** PANI **b** PANI- $CuFe_2O_4$ composite and **c** $CuFe_2O_4$

ascribe to the periodicity being parallel and perpendicular to the polymer chains. This suggests that the constitution of PANI exists in a semi crystalline form similar to emeraldine salt. The current results found can be confirmed using the preceding studies and documentations of the previous research and reports [4, 19]. From Fig. 5(b), it can be noted that the XRD pattern of the composite is related to that of ferrite with a faint peak (111) of PANI proving the predominance of ferrite particles and thereby verifying the interfacial interaction between PANI and the ferrite [19, 29].

The XRD pattern of $CuFe_2O_4$ (Fig. 5c) indicates peaks at 2θ = 19°, 31°, 35.24°, 38.40°, 44°, 53° and 62° that correspond to (111), (220), (311), (222), (400), (422) and (440) planes in tune with the standard joint commission PDS File No.25–0283 and also with the findings published in preceding research affirming that the synthesized $CuFe_2O_4$ has a single-phase cubic spinel structure with Fd3m space group [30].

However, the fact that the two other peaks of polyaniline (Fig. 5a) are not visible, prove that the ferrite particles restrain the growth of PANI to form a bulk polymer [25, 31]. This further reveals that structural similarity of the composite with that of the ferrite is rooted into PANI matrix and is ineffective to the ferrite's crystalline behavior [19, 32]. By Scherrer formula [33] as indicated in Eq. 1, at about 36° one can notice a sharp pronounced peak and the dimension for crystallite '*t*' is achieved around 12 nm and 20 nm for both the ferrite and the composite material.

$$t = \frac{k\lambda}{b\cos\theta} \tag{1}$$

4.3 Scanning electron microscopy

Figure 6 shows the scanning electron microscopy (SEM) image of the prepared PANI, PANI-$CuFe_2O_4$ composite and $CuFe_2O_4$. The SEM image in (Fig. 6a) outlines a well granular non-porous and agglomerated morphology with a homogeneous surface for PANI [34]. Figure 7b reveals that the highly agglomerated, uneven well-connected grains consisting of several pores which were very beneficial for adsorption of LPG molecules and the PANI particles serve as a cover on the surface of the ferrite particles. This kind of morphology promotes the formation of p–n junction creating an environment on the composite sample for the adsorption of gases directing gas diffusion into the junction there by making it desirable for gas sensing applications. There have been several citations of composites in recent studies with such identical morphological features [35–37]. The SEM image in Fig. 6 (c) establishes $CuFe_2O_4$ to be spongy structures consisting of several agglomerated particles and many are formed.

5 LPG sensing studies

The interaction of the composite PANI-$CuFe_2O_4$ with LPG was confirmed by a change in resistance when LPG was added into the chamber, followed by a return to the initial resistance when LPG was removed. The LPG sensing response of the composite has been studied at room temperature for different gas concentrations (ppm) scaling from 100–1200 ppm using fractional base line manipulation [38, 39] as per Eq. (2).

$$S(\%) = \frac{|R_{air} - R_{gas}|}{R_{air}} \text{X100} \tag{2}$$

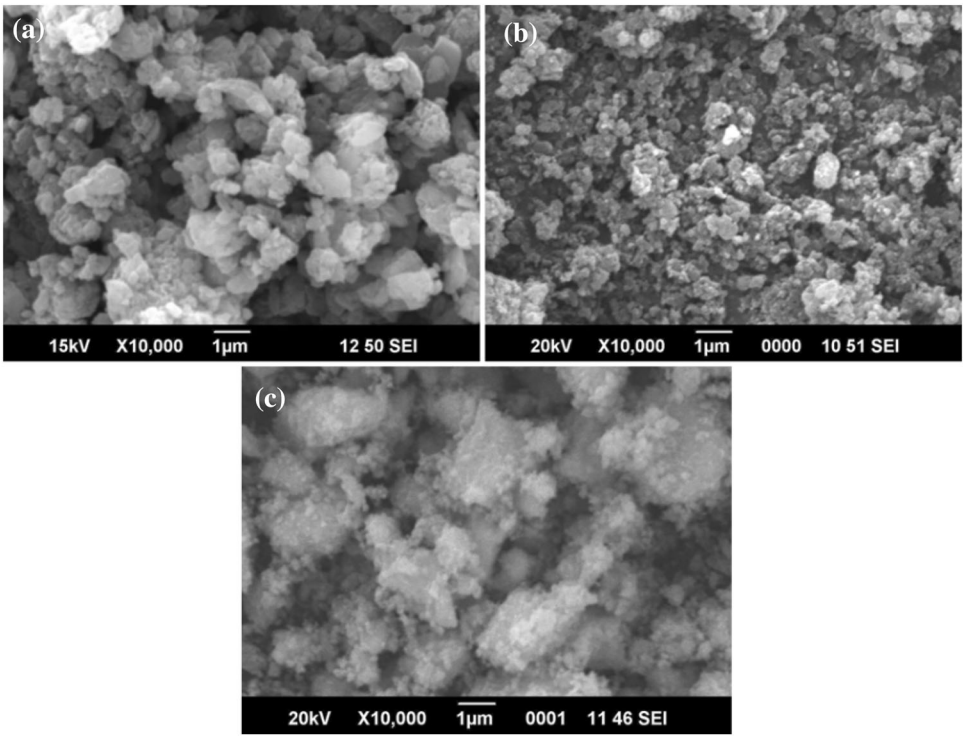

Fig. 6 SEM images of **a** PANI, **b** PANI- $CuFe_2O_4$ composite **c** $CuFe_2O_4$

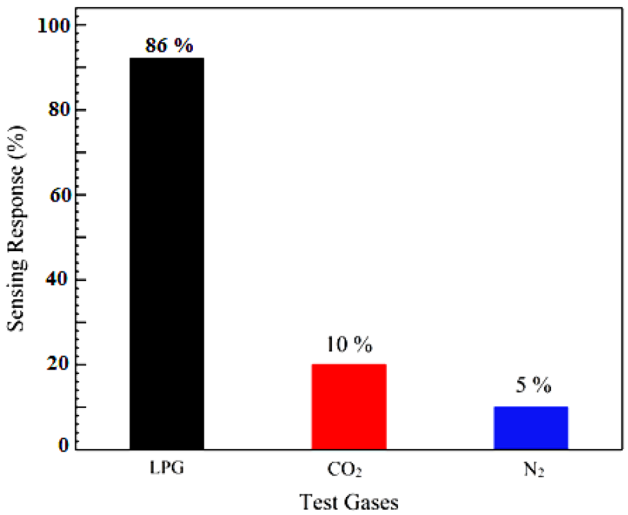

Fig. 7 Sensing response of PANI-$CuFe_2O_4$ composite for LPG, CO_2 and N_2 gases

where, R_{air} is the initial equilibrium resistance in presence of air and R_{gas} is the resistance in presence of the target gas of the sensing material.

Initially at room temperature, the sensing response of the composites was assessed for LPG (86%), CO_2 (10%), and N_2 (5%) gases at gas concentration of 764 ppm and it was found that the relative sensing response of the composite was found higher for LPG as shown in Fig. 7. So, further investigations on sensing by the composite was performed with LPG. Various concentrations of LPG were introduced into the chamber and corresponding resistance were recorded and sensing responses were calculated. The resulting plots of sensing response and also transient sensing response of the composite to various LPG concentrations. From the plot it can be seen that, at room temperature the sensing response of PANI and the composite to be varying for concentrations of LPG from 100–1200 ppm. From the following experimental analysis it can be recognized that a significant refinement of about 86% by the PANI-$CuFe_2O_4$ composite in LPG sensing response in comparison to the infirm sensing response of pristine PANI of 5% [3, 13] because due to high surface area, porosity and irregular cracks contributes more active sites which reveals from SEM (Fig. 7b) studies [40], Also, with the increase in concentration, the sensing response also consistently increases and the film of the composite was found sensitive for a low LPG concentration of 100 ppm [21, 41, 42]. Further, it is found that the resulting sensing response curve to be linear in the beginning from 764 ppm with a maximum sensing response of PANI–$CuFe_2O_4$ nanocomposite is 86% and then it becomes saturated. This observed saturation is because of multilayers of LPG on the

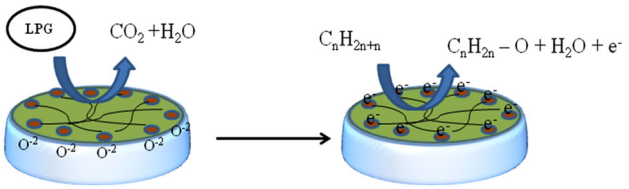

Fig. 8 Shows the LPG sensing mechanism of PANI-$CuFe_2O_4$ composite

composite being completely blocked by the sensing sites [21, 42–44].

The LPG sensing mechanism explain based on the two factors such as absorption of reduction gases on the composite surface and reduction of LPG gases into CO_2 and H_2O as shown in Fig. 8. The excess of oxygen in metal oxide provides O^{2-} charges on the composites materials which generates lot of free electron the composite surface. When LPG gas comes in contact over composites it reduce in to carbon dioxide and liberate water molecules. The linear segment of the sensing response characteristic can be explained with the help of energy band diagram drawn using measured values of band gap energies of PANI (2.52 eV) and $CuFe_2O_4$ (2.55 eV) and illustrated in Fig. 9. The mechanism of sensing can be understood interms of change in width of depletion layer that has formed between *p*-type PANI and *n*-type $CuFe_2O_4$ during the formation of the composite. Referring to the SEM image (Fig. 9b), the composites has open porous structure with an increased surface area where in the ferrite particles are embedded in the PANI matrix effectually form a *p*–*n* junction barrier layer between them. Consequently, on introducing a reducing gas such as LPG, into the chamber, it favorably gets adsorbed onto PANI and further liberates electrons upon interacting with its π electron network. This results in formation of more accepter ions on the *p*-side of the junction, thereby broadening the space-charge layer. Thus, the negatively charged O-ions of the ferrite drift from *n*-side of the junction toward the *p*-side expanding the depletion depth as shown in Fig. 9(c). This results in decrease of carrier accumulation at the junction and increase of the barrier height, further effecting the increase in the composite resistance [9, 45].

Figure 10 shows the change in resistance as a function of time when the LPG gas turned on and off for PANI and PANI PANI-$CuFe_2O_4$ composite. It is observed that the LPG gas absorbed at the initial concentration is high and reach at the peak

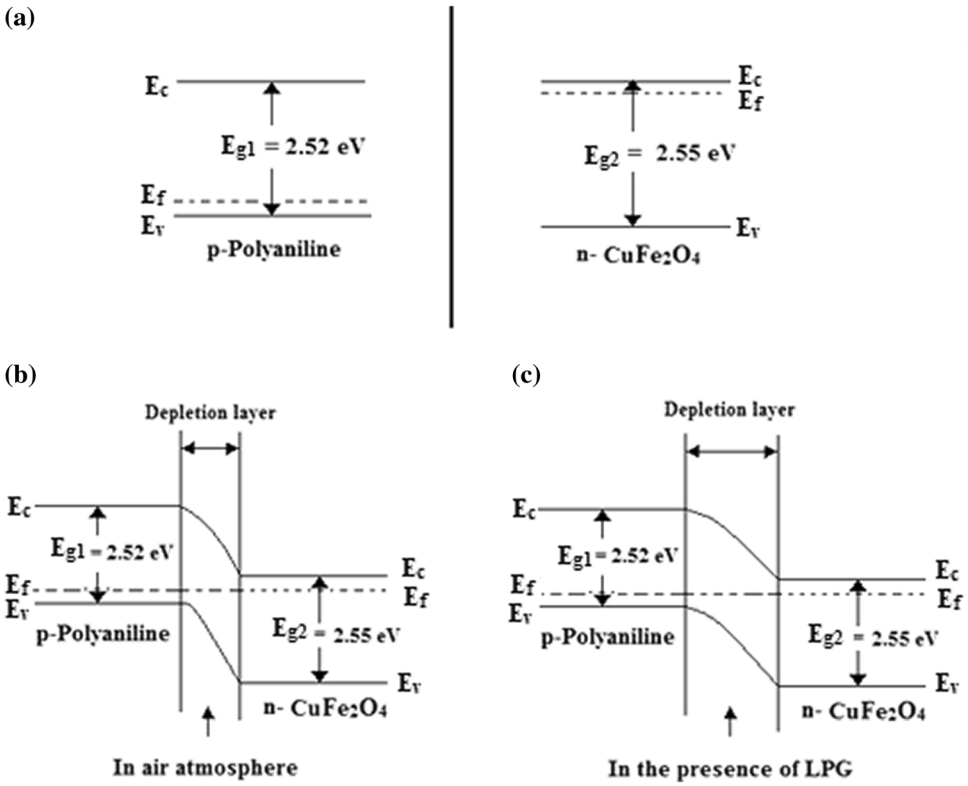

Fig. 9 Presents the proposed diagram view of energy band diagram for **a** individual PANI and $CuFe_2O_4$ **b** PANI-$CuFe_2O_4$ composite in the presence of air and **c** PANI-$CuFe_2O_4$ composite in presence of LPG

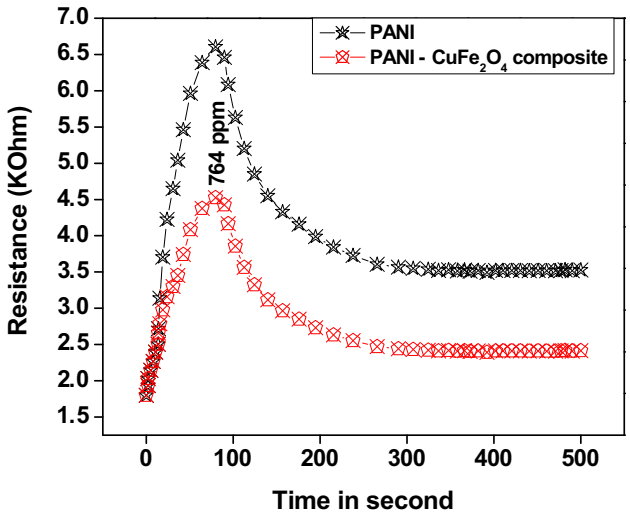

Fig. 10 Shows the change in resistance as a function of time

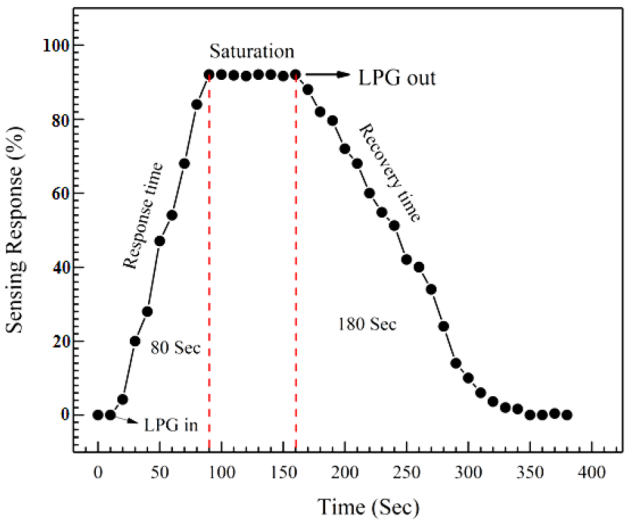

Fig. 11 Represents the response and recovery characteristic curve of PANI- $CuFe_2O_4$ composite to 1000 ppm of LPG

resistance at 764 ppm in 80 s. Later when LPG gas is turned off the resistance of the decreases may be due to the surface saturation of the PANI and its composite. The change in resistance may occurs due to the reduction of LPG gas on the PANI-$CuFe_2O_4$ composite results decrease in the free electron charge carrier on its surface and higher grain boundaries between the polyaniline. The composite elucidate the lower change in resistance and higher absorption capacity of LPG gas may be due to the formation of p-n heterojunctions between the PANI and $CuFe_2O_4$ particles results extended of chain length occurs in composite.

The Response time and recovey time are some essential factors which are vital to determine the feasibleness of devising the composites to function as LPG sensor [9, 46].

Figure 11 shows the composite's response and recovery characteristic curves at 1000 parts per million of LPG. When the gas was injected into the chamber, the composite demonstrated a very quick response time of 80 s, and a recovery period of 180 s when the gas was removed. In order to understand, the high LPG sensing performance of PANI-$CuFe_2O_4$ composite prepared by in-situ chemical polymerization method, its sensing response, response time, and recovery times were compared to those reported in earlier literatures of PANI/inorganic nanocomposite are given Table 1 [47–49]. The composite was also found to be stable in sensing over a one-month period when tested for 500 ppm and 1000 ppm of LPG (Fig. 12), with a negligible degradation of 3.5% in sensing response. Thus LPG sensor using these composites is having advantages such as the working temperature can be brings down to room temperature, leads to increases in the life time of sensor elements and the interfering gases are less active when compared to LPG. Thus the sensor has good selectivity for LPG. A prototype of the device is also fabricated and experimental trails under progress for practical outdoor as well as domestic applications.

6 Conclusions

The Polyaniline–$CuFe_2O_4$ nanocomposites with different weight percentages have been prepared by in-situ polymerization and the prepared nanocomposites spin coated over glass to fabricate of an LPG sensing device which outperforms in terms of efficiency. FTIR spectra of the nanocomposites revels a shift in the characteristic peaks at higher wave number due to the π–π interaction of PANI and $CuFe_2O_4$ nanoparticles. The crystalline nature of the nanocomposite and nanostructure was confirmed by XRD investigation. SEM analysis revealed that granular agglomerated structure of PANI nanocomposites. The change in resistance confirms the higher absorption of LPG gas due to the formation of p-n heterojunctions between the PANI and $CuFe_2O_4$ nanoparticles. It is also

Table 1 Earlier literatures on the sensing performance of PANI/inorganic nanocomposite for LPG sensor

Composite	Fabrication method	Target gas	Max. Concentration of LPG	Sensing response	Response time (s)	Recovery time (s)	Operating temp. (° C)	Ref
PANI/TiO_2	In-situ chemical polymerization	LPG	0.4 vol%	43.2%	76	95	Room temperature (RT)	[47]
PANI-Nb_2O_5	In-situ chemical polymerization	LPG	500 ppm	45.21%	30	50	RT	[49]
PANI-$CdFe_2O_4$	In-situ chemical polymerization	LPG	1000 ppm	50.83%	50	110	RT	[21]
PANI-NF	In-situ chemical polymerization	LPG	700 ppm	57%	50	200	RT	[4]
p-polyaniline/n-CdTe	Electrodeposition technique	LPG	0.16 vol%	67.7%	300	600	RT	[10]
p-polyaniline/n-PbS	Electrodeposition technique	LPG	780 ppm	70%	–	–	RT	[9]
p-polyaniline/Cu_2ZnSnS_4	Electrodeposition technique	LPG	780 ppm	79%	120	125	RT	[11]
n-CdS/p-polyaniline	Electrodeposition technique	LPG	1040 ppm	80%	210	105	RT	
Polyaniline-$CuFe_2O_4$	In-situ chemical polymerization	LPG	764 ppm	86%	80	180	RT	Present work

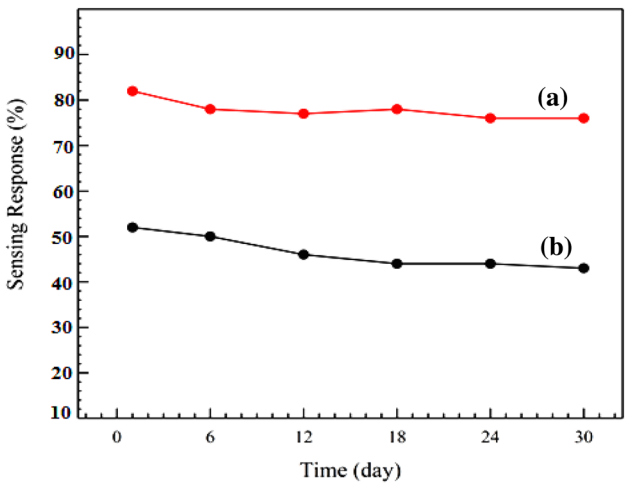

Fig. 12 Shows stability response of PANI- $CuFe_2O_4$ composite at **a** 1000 ppm and **b** 500 ppm of LPG concentration

important to note that the porous morphology of the nanocomposite is particularly favorable for LPG adsorption. A simple LPG sensor that works at room temperature and is made entirely of spin coated PANI-$CuFe_2O_4$ nanocomposite structure was found to have a maximum sensing response of 86% at 764 ppm of LPG. The energy band diagram was used to explain the sensing mechanism. Over the course of one month, the sensor was determined to be stable, with response and recovery times of 80 and 180 s, respectively. As a result, the composite has the potential to be an effective LPG sensor.

Author contribution

SK and AR are responsible for the designing of the work, prepared the materials and completed the initial drafting of the manuscript. **AP** and **AM** are contributed in the characterizations and analysis of the composite data. **NB** is contributed in the final drafting, editing and analyzing the spectra.

Data availability

Data underlying the results presented in this paper are not publicly available at the time of publication, which may be obtained from the authors upon reasonable request.

Declarations

Conflict of interest This is to inform you that author and co-authors do not have any financial or non-financial and even direct or indirect conflict of interest.

References

1. A.G. MacDiarmid, Semiconducting and metallic polymers: The fourth generation of polymeric materials. Synth. Met. **125**, 11–22 (2002)
2. S. Srivastava, S.S. Sharma, S. Kumar, S. Agarwal, M. Singh, Y.K. Vijay, Characterization of gas sensing behavior of multi walled carbon nanotube polyaniline composite films. Int. J. Hydrogen Energy. **34**, 8444–8450 (2009)
3. B.B. Ravikiran, U. Deepak, M. Sandip, J.C. Vyas, R. Sharma, Study of room temperature LPG sensing behavior of polyaniline thin film synthesized by cost effective oxidative polymerization technique. J. Mater Sci: Mater. Electron. **26**, 5065–5070 (2015)
4. S. Kotresh, Y.T. Ravikiran, S.C. Vijayakumari, S. Thomas, Interfacial p–n heterojunction of polyaniline–nickel ferrite nanocomposite as room temperature liquefied petroleum gas sensor. Compos Interfaces **24**, 549–561 (2017)
5. B. Mu, W. Zhang, A. Wang, Template synthesis of graphene/polyaniline hybrid hollow microspheres as electrode materials for high-performance supercapacitor. J Nanopart Res. **16**, 2432–2443 (2014)
6. Y. Jafari, S.M. Ghoreishi, M. Shabani-Nooshabadi, Electrochemical deposition and characterization of polyaniline-graphene nanocomposite films and its corrosion protection properties. J Polym Res. **23**, 91–103 (2016)
7. R.H. Lee, C.H. Chi, Y.C. Hsu, Platinum nanoparticle/self-doping polyaniline composite based counter electrodes for dye-sensitized solar cells. J Nanopart Res. **15**, 1733–1747 (2013)
8. S. Shin, J. Kim, Y.H. Kim, S.I. Kim, Enhanced performance of organic light-emitting diodes by using hybrid anodes composed of graphene and conducting polymer. Curr Appl Phys **13**, S144–S147 (2013)
9. S.V. Patil, R.N. Bulakhe, P.R. Deshmukh, N.M. Shinde, C.D. Lokhande, LPG sensing by p-polyaniline/n-PbS heterojunction capacitance structure. Sens. Actuators, A **201**, 387–394 (2013)
10. S.S. Joshi, T.P. Gujar, V.R. Shinde, C.D. Lokhande, Fabrication of n-CdTe/p-polyaniline heterojunction-based room temperature LPG sensor. Sens. Actuators, B **132**, 349–355 (2008)
11. S.J. Patil, A.C. Lokhande, A.A. Yadav, C.D. Lokhande, Polyaniline/Cu_2ZnSnS_4 heterojunction based room temperature LPG sensor. J. Mater. Sci.: Mater. Electron. **27**, 7505–7508 (2016)
12. D.S. Dhawale, R.R. Salunkhe, U.M. Patil, K.V. Gurav, A.M. More, C.D. Lokhande, Room temperature liquefied petroleum gas (LPG) sensor based on P-polyaniline/n-TiO_2 heterojunction. Sens. Actuators, B. **134**, 988–992 (2008)
13. Y.T. Ravikiran, S. Kotresh, S.C. Vijayakumari, S. Thomas, Liquid petroleum gas sensing performance of polyaniline-carboxymethyl cellulose composite at room temperature. Curr. Appl. Phys. **14**, 960–964 (2014)
14. S. Singh, A. Singh, B.C. Yadav, P. Tandon, Synthesis, characterization, magnetic measurements and liquefied petroleum gas sensing properties of nanostructured cobalt ferrite and ferric oxide. Mater. Sci. Semicond. Process. **23**, 122–135 (2014)
15. E. Ranjith Kumar, R. Jayaprakash, G. Sarala Devi, P. Siva Prasada Reddy, Magnetic, dielectric and sensing properties of manganese substituted copper ferrite nanoparticles. J. Magn. Magn. Mater. **355**, 87–92 (2014)
16. S. Sulthana, M.Z. Rafiuddin, K.U. Khan, Synthesis and characterization of copper ferrite nanoparticles doped Polyaniline. J Alloys Compd. **535**, 44–49 (2012)
17. Z.X. Sun, F.W. Su, W. Forsling, P.O. Samskog, Surface Characteristics of magnetite in aqueous suspension. J. Colloid. Interface Sci. **197**, 151–159 (1998)
18. J. Jiang, L. Li, F. Xu, Polyaniline–LiNi ferrite core–shell composite: Preparation, characterization and properties. Mater Sci Eng A **456**, 300–304 (2007)
19. V.A. Zhuravlev, R.V. Minin, V.I. Itin, I.Y. Lilenko, Structural parameters and magnetic properties of copper ferrite nanopowders obtained by the sol-gel combustion. J Alloys Compd. **692**, 705–712 (2017)
20. E.R. Kumar, R. Jayaprakash, S. Devi, S.P. Reddy, Magnetic, dielectric and sensing properties of manganese substituted copper ferrite nanoparticles. J. Magn. Magn. Mater. **355**, 87–92 (2014)
21. S. Kotresh, Y.T. Ravikiran, S.K. Tiwari, S.C. Vijaya Kumari, Polyaniline–cadmium ferrite nanostructured composite for room-temperature liquefied petroleum gas sensing. J. Electron. Mater. **46**, 5240–5247 (2017)
22. S. Quillard, G. Louarn, S. Lefrant, A.G. MacDiarmid, Vibrational analysis of polyaniline: A comparative study of leucoemeraldine, emeraldine, and pernigraniline bases. Phys. Rev. B: Condens. Matter **50**, 12496–12508 (1994)
23. D. Geethalakshmi, N. Muthukumarasamy, R. Balasundaraprabhu, Effect of dopant concentration on the properties of HCl–doped PANI thin films prepared at different temperatures. Optik **125**, 1307–1310 (2014)
24. P.C. Wang, Y. Dan, L.H. Liu, Effect of thermal treatment on conductometric response of hydrogen gas sensors integrated

with HCl-doped Polyaniline nanofibers. Mater. Chem. Phys. **144**, 155–161 (2014)
25. X. Li, G. Wang, X. Li, Surface modification of nano–SiO2 particles using Polyaniline. Surf Coat. Technol. **197**, 56–60 (2005)
26. R.D. Waldron, Infrared spectra of ferrites. Phys Rev **99**, 1727–1735 (1955)
27. X. Zhang, M. Feng, R. Qu, H. Liu, L. Wang, Z. Wang, Catalytic degradation of diethyl phthalate in aqueous solution by persulfate activated with nano-scaled magnetic $CuFe_2O_4$/MWCNTs. Chem. Eng. J. **301**, 1–11 (2016)
28. M. Khairy, Synthesis, characterization, magnetic and electrical properties of polyaniline/$NiFe_2O_4$ nanocomposite. Synth Met **189**, 34–41 (2014)
29. R.M. Khafagy, Synthesis, characterization, magnetic and electrical properties of the novel conductive and magnetic polyaniline/$MgFe_2O_4$ nanocomposite having the core–shell structure. J Alloys Compd. **509**, 9849–9857 (2011)
30. S. Briceno, H.D. Castillo, V. Sagredo, W. Bramer-Escamilla, P. Silva, Structural, catalytic and magnetic properties of $Cu_{1-x}Co_xFe_2O_4$. Appl. Sur. Sci. **263**, 100–103 (2012)
31. S. Min, F. Wang, Y. Han, An investigation on synthesis and photocatalytic activity of polyaniline sensitized nanocrystalline TiO_2 composites. J Mater Sci. **42**, 9966–9972 (2007)
32. A.T. Mane, S.T. Navale, S. Sen, D.K. Aswal, S.K. Gupta, V.B. Patil, Nitrogen dioxide (NO_2) sensing performance of p-polypyrrole/n-tungsten oxide hybrid nanocomposites at room temperature. Org. Electron. **16**, 195–204 (2015)
33. A.L. Patterson, The scherrer formula for X-Ray particle size determination. Phys. Rev. B **56**, 978–982 (1939)
34. M. Faisal, S. Khasim, Ku–band EMI shielding effectiveness and dielectric properties of polyaniline–Y_2O_3 composites. Polym. Sci. Ser. A **56**, 366–372 (2014)
35. H. Hou, G. Xu, S. Tan, Y. Zhu, A facile sol-gel strategy for the scalable synthesis of $CuFe_2O_4$ nanoparticles with enhanced infrared radiation property: Influence of the synthesis conditions. Infrared Phys. Technol. **85**, 261–265 (2017)
36. R.K. Sonker, B.C. Yadav, Development of Fe_2O_3-PANI nanocomposite thin film based sensor for NO_2 detection. J. Taiwan Inst. Chem Eng. **77**, 276–281 (2017)
37. B. Senthilkumar, K. Vijaya Sankar, C. Sanjeeviraja, R. Kalai Selvan, Synthesis and physico-chemical property evaluation of PANI-$NiFe_2O_4$ nanocomposite as electrodes for supercapacitors. J. Alloys Compd. **553**, 350–357 (2013)
38. T. Sen, N.G. Shimpi, S. Mishra, R. Sharma, Polyaniline/–Fe2O3 nanocomposite for room temperature LPG sensing. Sens. Actuators B **190**, 120–126 (2014)
39. R.V. Barde, Preparation, characterization and CO_2 gas sensitivity of polyaniline doped with sodium superoxide (NaO_2). Mater. Res. Bull. **73**, 70–76 (2016)
40. S.T. Navale, G.D. Khuspe, M.A. Chougale, V.B. Patil, Camphor sulfonic acid doped PPy/α-Fe_2O_3 hybrid nanocomposites as NO_2 sensors. RSC Adv. **4**, 27998–28004 (2014)
41. X. Yang, L. Li, F. Yan, Polypyrrole/silver composite nanotubes for gas sensors. Sens. Actuators B **145**, 485–500 (2010)
42. S. Kotresh, Y.T. Ravikiran, S.C. Vijaya Kumari, T. Chandrasekhar, C.H.V.V. Ramana, S. Thomas, Solution-based spin cast processed polypyrrole/niobium pentoxide nanocomposite as room temperature liquefied petroleum gas sensor. Mater Manuf Processes **31**, 1976–1982 (2016)
43. S.S. Barkade, D.V. Pinjari, U.T. Nakate, A.K. Singh, P.R. Gogate, J.B. Naik, S.H. Sonawane, A.B. Pandit, Ultrasound assisted synthesis of polythiophene/SnO_2 hybrid nanolatex particles for LPG sensing. Chem. Eng. Process. **74**, 115–123 (2013)
44. A. Parveen, A. koppalkar, A.S. Roy, Liquefied Petroleum Gas Sensing of Polyaniline-Titanium Dioxide Nanocomposites. Sens. Lett. **11**, 242–248 (2013)
45. M. Khairy, Polyaniline-$Zn_{0.2}Mn_{0.8}Fe_2O_4$ ferrite core-shell composite: Preparation, characterization and properties. J. Alloys Comp. **608**, 283–291 (2014)
46. M. Singh, B.C. Yadav, U. Kumar, R. Ashok Ranjan, M.K. Srivastava, Fabrication of nanostructured lead-free bismuth sodium titanate thin film and its liquefied petroleum gas sensing. Sens. Actuators, A **301**, 111765 (2020)
47. A.A. Omar, S. Khasim, A. Roy, A. Pasha, Highly conductive Polyaniline/graphene nano-platelet composite sensor towards detection of toluene and bezene gases. Appl. Phys. A **125**, 1–12 (2019)
48. M. Moradian, S. Nasirian, Structural and room temperature gas sensing properties of polyaniline/titania nanocomposite. Org. Electron. **62**, 290–297 (2018)
49. S. Kotresh, Y.T. Ravikiran, S.C. Vijayakumari, Ch.V.V. Ramana, K.M. Batoo, Solution based-spin cast processed LPG sensor at room temperature. Sens. Actuators, A, 263, 687–692 (2017).